

Voltage-tunable quantum dots on silicon

J. Alsmeier, E. Batke, and J. P. Kotthaus*

Institut für Angewandte Physik, Universität Hamburg, Jungiusstrasse 11, D-2000 Hamburg 36, Federal Republic of Germany

(Received 10 October 1989)

Employing electrostatic confinement with a dual-gate device we realize periodic arrays of electron dots on Si widely tunable in diameter and electron number. From far-infrared transmission studies of dimensional resonances, we deduce dot diameters down to 40 nm for as little as 20 electrons in quantum states spaced by more than 5 meV. Excitation energies as well as mode dispersions in finite magnetic fields are found to strongly depend on the strength and the shape of the lateral confining potential. A detailed analysis of the oscillator strengths indicates a direct effect of strong quantum confinement.

The high-frequency response of laterally bound electron layers has been investigated both in classically confined quasi-two-dimensional (2D) systems¹⁻³ and, more recently, in quantum confined systems that exhibit either quasi-one-dimensional^{4,5} (1D) or quasi-zero-dimensional⁶ (0D) properties. In particular, 1D inversion channels realized on GaAs, InSb, and Si have been extensively studied.^{4,5,7} Very recently electrons have been confined to 0D quantum dots on GaAs (Refs. 8-10) and InSb.⁶ Here we study the high-frequency response of periodic arrays of dots on Si containing few (20-350) inversion electrons. Significant quantum confinement on silicon can only be expected with dot diameters W well below 100 nm. To meet this requirement we prepare a dual-gate structure which allows us to electrostatically define a wide range of dot diameters between 40 and 150 nm. Moreover, the main advantage of such a device is the continuous and nearly independent tunability of the depth of the lateral confining potential, the dot diameter W , and the electron number N_0 . This enables us to study the high-frequency response of dot arrays on Si in the transitory regime between classical and quantum confinement.

Figure 1 shows a schematic cross section of our dual-gate metal-oxide-silicon device. The bottom gate is a semitransparent NiCr mesh sandwiched between a thermal SiO₂ layer, grown on (100) *p*-type Si with a specific resistivity of 20 Ω cm at 300 K, and a plasma-enhanced chemical-vapor deposition (PECVD) SiO₂ layer with a thin continuous NiCr layer of $R_g \approx 1$ kΩ/□ on top. The scanning electron micrograph shows a top view of the bottom gate. The mesh has a periodicity of $a = 400$ nm with circularly shaped openings of diameter $t \approx 150$ nm. Different voltages V_{gt} and V_{gb} are applied between a substrate contact and the top and bottom gates, respectively. In the presence of band-gap radiation electron dots are induced at the Si-SiO₂ interface underneath the openings of the bottom gate via V_{gt} . While V_{gt} essentially determines N_0 , V_{gb} serves to isolate the dots and to continuously vary the depth of the lateral confining potential from zero to a value exceeding the band gap of Si. As demonstrated below at fixed V_{gt} and V_{gb} , the electronic diameter of the dots W can be further reduced via a substrate-bias voltage V_{SB} which is added to V_{gt} in the dark and does not significantly change N_0 . This enhances the depletion

charge N_{depl} and thus squeezes the dots, as has been previously demonstrated for narrow electron wires on Si.¹¹

The electronic response of the dot array is advantageously studied with far-infrared spectroscopy at 2 K.^{1,4} We measure the relative change in transmission

$$-\Delta T/T = [T(0) - T(\sigma(\omega))]/T(0),$$

where $\sigma(\omega)$ is the effective high-frequency conductivity of the electrons in the dot array. In the small signal approximation appropriate here

$$-\Delta T/T \approx [2 \operatorname{Re}(\sigma(\omega))/\epsilon_0 c]/(1 + \sqrt{\epsilon + \sigma_g/\epsilon_0 c})$$

is proportional to the real part of this conductivity with

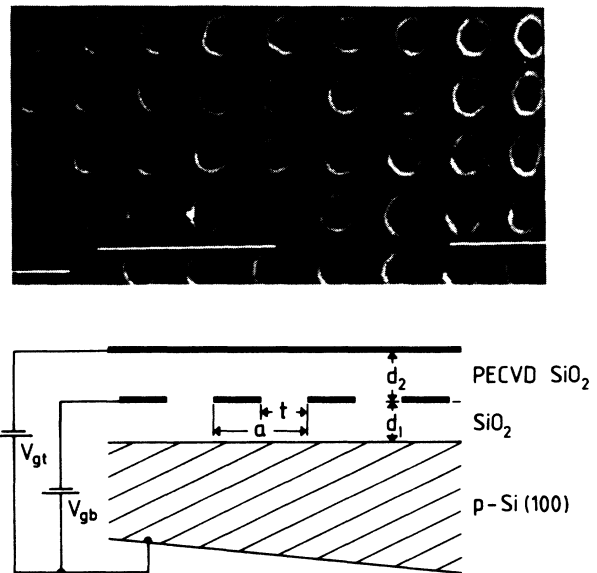


FIG. 1. Schematic cross section of a dual-gate device on Si. The top gate is a homogeneous 5-nm-thick NiCr layer, whereas the bottom gate is a NiCr mesh of periodicity $a = 400$ nm embedded between a thermal ($d_1 = 50$ nm) and a PECVD ($d_2 = 150$ nm) SiO₂. The scanning electron micrograph with 1- μ m marker shows a top view of the bottom gate indicating circularly mesh opening with diameter $t \approx 150$ nm.

the dielectric constant of Si $\epsilon = 11.5$ and an effective sheet conductivity $\sigma_g = (1 \text{ k}\Omega)^{-1}$ for both gates. In order to determine N_0 from the experimental line shape we approximate the high-frequency conductivity by a classical expression

$$\sigma(\omega) \approx \sigma_{\text{class}}(\omega) = \sigma_0 / [1 + (\omega_0^2/\omega - \omega)^2 \tau^2]$$

with $\sigma_0 = (N_0/a^2)(e^2\tau/m^*)$ for electrons confined in a parabolic potential.⁶ From fits to the line shape a phenomenological scattering time $\tau \approx 0.2 \times 10^{-12}$ s, nearly independent of N_0 , is obtained. Thus the resonance amplitude $-\Delta T/T(\omega = \omega_0)$ gives a direct, absolute measure of the average electron density N_0/a^2 .

Figure 2(a) illustrates the high-frequency response at zero magnetic field for different V_{gt} and two different values of V_{SB} . The confined electrons yield a strong dimensional resonance which shifts weakly to lower energies for decreasing V_{gt} and thus decreasing N_0 . This demon-

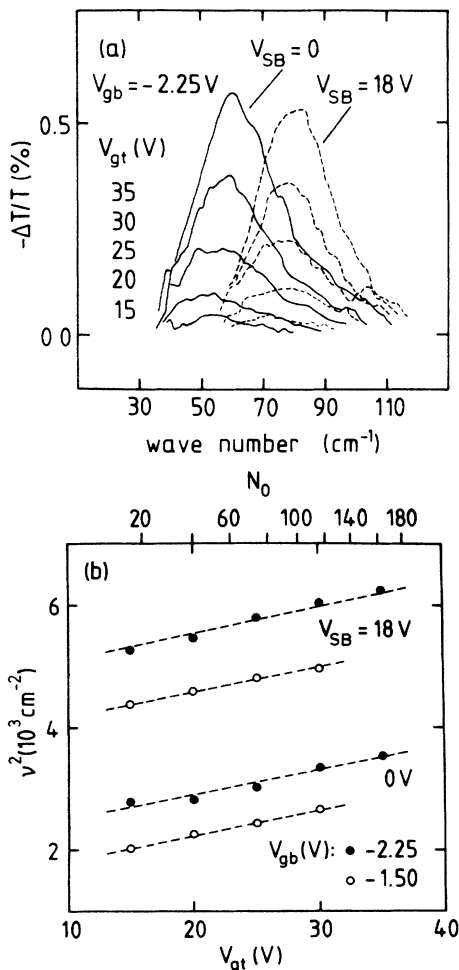


FIG. 2. (a) Dimensional resonances of a periodic array of electron dots on (100) p-type Si as seen in the relative change in transmission $-\Delta T/T$. Parameters are the top gate (V_{gt}), the bottom gate (V_{gb}), and the substrate bias (V_{SB}) voltage, respectively (solid traces, $V_{SB}=0$; dashed traces, $V_{SB}=18$ V). (b) Squared resonance positions at different V_{SB} and V_{gb} vs top gate voltage V_{gt} . The dashed lines are guides to the eye. The electron numbers N_0 displayed on top are only valid for $V_{gb} = -2.25$ V (solid circles).

strates the importance of quantum confinement at least for small N_0 , where the dimensional resonance in a classically confined system approaches zero frequency.¹ With increasing V_{SB} the resonance frequency increases strongly, indicating an increased confinement. Note that the number of electrons in a dot varies only marginally with V_{SB} as judged from the oscillator strength.

For the devices studied here, the flat band voltage as determined from the quasiaccumulation threshold for the bottom gate is $V_{gb} \approx -2$ V. At $V_{gb} \leq -1$ V and $V_{gt} \geq 10$ V electron dots are induced in the presence of a pulse of band-gap radiation via V_{gt} , whereas the depth of the confining potential can be adjusted with V_{gb} between -1 and -2.25 V from nearly zero to a value exceeding the band gap of Si. At $V_{gb} = -2.25$ V, free holes are induced at the Si-SiO₂ interface underneath the bottom gate, surrounding the electron dots and forming a lateral “nipi” structure. For the latter case fringing field effects strongly reduce the dot diameter.¹² This is reflected in the measured resonance frequencies. The squared resonance frequencies are displayed versus V_{gt} for two different bottom-gate and substrate-bias voltages in Fig. 2(b). For $V_{gb} = -2.25$ V (solid circles) the approximate electron number N_0 , as extracted from the oscillator strength at zero magnetic field, is entered in the top of Fig. 2(b) in a nonlinear scale. For $V_{gb} = -1.5$ V (open circles) N_0 depends linearly on V_{gt} and is, for $N_0 \approx 17(V_{gt} - 10)$ V, typically a factor of 3 higher than for $V_{gb} = -2.25$ V. Varying V_{gb} and V_{SB} , the resonance frequency of the dimensional resonance can easily be tuned by a factor of 2 even at constant V_{gt} . The dashed lines are guides to the eye and indicate a linear dependence of the squared resonance energies on V_{gt} . Extrapolating the squared resonance energies to the conductivity threshold at $V_{gt} \approx 10$ V we obtain finite offsets. This is in contrast to the behavior expected for a classically confined disk with depolarization frequency $\omega_d^2 \propto N_0/W^3$.¹ Our resonances represent transitions between quantum confined electron states with transition energy $\hbar\omega_0 = \hbar(\omega_{0D}^2 + \bar{\omega}^2)^{1/2}$, where $\hbar\omega_{0D}$ is the separation between 0D quantum states and $\hbar\bar{\omega}$ a collective shift. In principle, coupling between adjacent dots will affect the transition energies.¹³ Previously, we have demonstrated in a study of arrays of narrow electron channels using a qualitatively similar dual-gate device that the influence of coupling between adjacent electron systems is small, in particular, if the confining potential is sufficiently deep.⁵ This gives us confidence that such coupling can also be neglected here.

We obtain 0D quantum energy state separations at vanishing N_0 between about 5 and 9 meV, comparable to recent experiments on InSb.⁶ Since electrons on Si(100) have effective masses $m^* \approx 0.19m_e$ more than 1 order of magnitude larger than on InSb our dot diameters at the same N_0 are considerably smaller. From studies on InSb (Ref. 6) and theoretical calculations¹⁴ one can expect that the separation of quantum states depends little on N_0 for small N_0 . Assuming a parabolic lateral confining potential, we thus calculate with the above energy separations at $N_0 \approx 20$, equivalent to $N=4$ occupied 0D states, electronic dot diameters $W = 2(2\hbar N/m^*\omega_{0D})^{1/2}$ between 37 and 50 nm. Using the classical approximation for the

highest N_0 values in Fig. 2, we estimate $W \approx 100$ nm for $V_{gb} = -2.25$ V, about a factor of 1.5 smaller than the geometrical value $t \approx 150$ nm.

In Fig. 3 we display the development of the dimensional resonances in a magnetic field B applied perpendicularly to the sample surface. Figure 3(a) shows resonances of dots with $N_0 \approx 350$ electrons in a shallow lateral confining potential, whereas Fig. 3(b) shows spectra for dots with $N_0 \approx 140$ and a strong lateral confinement. Previously, such spectra have been investigated in periodic arrays of classical disks on GaAs (Ref. 1) with $N_0 \approx 3 \times 10^4$ and of quantum dots on InSb (Ref. 6) with $N_0 \approx 3-20$, respectively. These experiments revealed two resonances with a mode dispersion for a parabolic confined electron system, namely

$$\omega_{\pm} = \pm \frac{\omega_c}{2} + \left[\left(\frac{\omega_c}{2} \right)^2 + \omega_0^2 \right]^{1/2}. \quad (1)$$

Here ω_+ describes a bulklike resonance, approaching the cyclotron frequency $\omega_c = eB/m^*$ of the unbound quasi-two-dimensional system in the high magnetic field limit, whereas ω_- is an edgelike mode decreasing in energy with increasing B . At vanishing magnetic field strength both resonances combine to form a single dimensional resonance dominated by depolarization in the classical extreme¹ and by quantum confinement in the quantum dot case. Comparing our experimental resonance positions with the mode dispersions of Eq. (1), we find deviations from the prediction $\omega_+ - \omega_- = \omega_c$. This is shown, for example, in Fig. 4 for dots with $80 \leq N_0 \leq 350$ at $V_{SB} = 0$ and $V_{SB} = 18$ V. At $V_{SB} = 0$ the experimental points of the upper mode are almost independent of N_0 , whereas the lower mode frequencies decrease in energy with decreasing N_0 . The dashed line in Fig. 4 is calculated for

$N_0 = 350$ with Eq. (1) and describes the experiment well. However, for $N_0 \leq 250$ we find a larger separation of $\omega_+ - \omega_-$ than predicted. This becomes most obvious as $\omega_+ - \omega_- - \omega_c > 0$, as shown in the inset of Fig. 4. The resonance position for the zero-field value is also lower than expected by the dashed curve. The closed symbols in Fig. 4 are obtained under an applied substrate-bias voltage which shrinks the dots and enhances the confinement. The solid lines are calculated for $N_0 = 80$ and 350 with the experimentally observed ω_0 and we obtain excellent agreement with the experiment. The mode behavior shown in Fig. 4 does not depend in a sensitive manner on the depth of the confining potential and is also qualitatively found for $V_{gb} = -2.25$ V. We attribute the observed mode behavior to reflect a softening of the walls of the confining potential resulting in a stronger effect on the edge resonance. For the same reason we believe the bulklike mode to deviate from the prediction of Eq. (1) as B approaches zero. However, this effect is of a classical nature and has been predicted in a similar form.¹⁵

The dashed lines in Fig. 3 are calculated values of $-\Delta T/T$ with a high-frequency magnetoconductivity given for classical electron disks in Ref. 16 and a phenomenological scattering time $\tau = 0.2 \times 10^{-12}$ s. In the classical ansatz a single τ rules both modes which has the meaning of a momentum relaxation time. The ratio of oscillator strengths S_+/S_- in the limit $\tau \rightarrow \infty$ is predicted to vary as $S_+/S_- = \omega_+/\omega_-$ with an amplitude ratio of $A_+/A_- = 1$ but B -dependent half-width $\Delta\omega_+/\Delta\omega_- = \omega_+/\omega_-$. This classical prediction for S_+/S_- is identical with the quantum-mechanical one for noninteracting electrons in a parabolic confinement assuming equal scattering mechanisms for both modes, whereas the quantum-mechanical model predicts $\Delta\omega_+/\Delta\omega_- = 1$.¹⁷

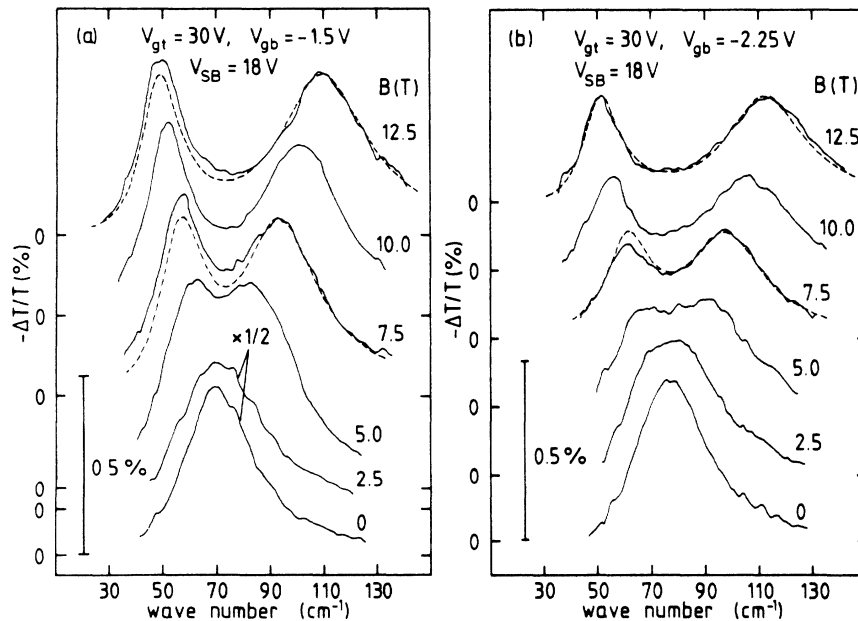


FIG. 3. Relative change in transmission $-\Delta T/T$ of an array of electron dots on Si at $V_{SB} = 18$ V in magnetic fields B applied perpendicularly to the sample surface. The dotted lines are calculated as discussed in the text. (a) Dots containing $N_0 \approx 350$ electrons at different B and $V_{gb} = -1.5$ V. (b) $N_0 \approx 140$ and $V_{gb} = -2.25$ V.

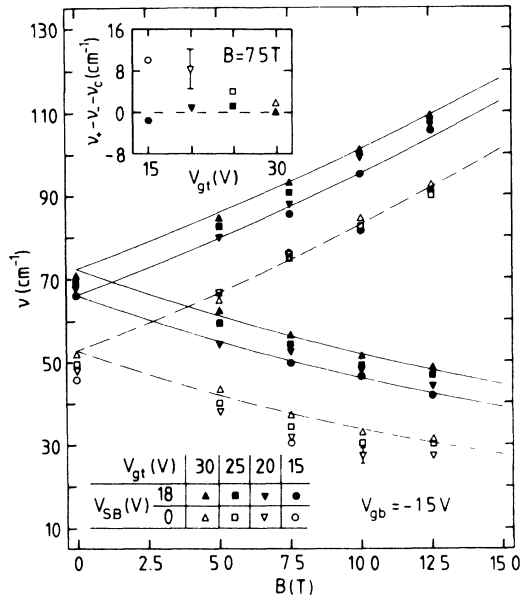


FIG. 4. Resonance positions for electron dots on Si vs magnetic field B at different $N_0 \approx 17 (V_{gt} - 10 \text{ V})$ and V_{SB} . Dashed and solid lines are calculated with Eq. (1). The separation of the resonance positions vs N_0 as discussed in the text is shown in the inset for $B = 7.5 \text{ T}$.

Experimentally, we observe significant deviations from both expectations, as shown in Figs. 3(a) and 3(b) for two regimes. Generally, for many electrons $N_0 \geq 250$ confined in a shallow potential where we expect a classical behavior [Fig. 3(a)] we find a larger oscillator strength of the lower mode and $A_+/A_- < 1$. This behavior is found to persist up to the highest magnetic fields studied here and is also found for electron disks with quite high electron numbers ($N_0 > 2500$).¹¹ In contrast, for dots with few electrons $20 \leq N_0 \leq 140$ confined in a deep potential [Fig. 3(b)] and for a medium magnetic field strength S_- is smaller than expected from above models, i.e., S_+/S_-

increases for decreasing electron number from $S_+/S_- \approx 1.3(\omega_+/\omega_-)$ at $N_0 = 140$ to $S_+/S_- \approx 1.5(\omega_+/\omega_-)$ at $N_0 = 50$. This becomes obvious in Fig. 3(b) with $A_- < A_+$. Since we lack a theory of the dynamic response of our system in the transition regime between classical and quantum confinement, we fit the individual modes with Lorentzian line shapes thus obtaining reliable relative oscillator strengths. The decrease of the amplitude A_- with respect to A_+ is expected for a quantum confined dot with noninteracting electrons. However, as B is increased S_+/S_- approaches ω_+/ω_- and $A_+/A_- = 1$ as shown in Fig. 3(b) at $B = 12.5 \text{ T}$. This happens in a magnetic field regime where the dot diameter W becomes larger than the cyclotron orbit diameter

$$2R_c = 2[(2n+1)\hbar/eB]^{1/2} \approx 2(2\pi N_S)^{1/2}\hbar/eB,$$

where $N_S = N_0/\pi(W/2)^2$ is the equivalent 2D density. Therefore, we conclude that the enhanced ratio of oscillator strengths S_+/S_- as well as the enhanced ratio of amplitudes A_+/A_- reflects the stronger quantum confinement.

In conclusion, we demonstrate that with a dual-gate device on Si one can create and electrostatically tune quantum dots with low electron numbers and electronic diameters that can be much smaller than the geometrical diameter defined by lithographic techniques. The structure enables us to carefully study the transition from the classical to the quantum regime and its effect on the oscillator strength and the resonance positions in a magnetic field. The latter show that a refined theoretical description is necessary for the dynamic response in such quantum structures.

We would like to thank Th. Ebelbauer, Unternehmensbereich der Philips, Hamburg for providing us with oxidized Si wafers, and acknowledge financial support by the Stiftung Volkswagenwerk and the Deutsche Forschungsgemeinschaft.

*Permanent address: Sektion Physik, Universität München, Geschwister-Scholl-Platz 1, 8000 München 22, Federal Republic of Germany.

¹S. J. Allen, Jr., H. L. Störmer, and J. C. M. Hwang, Phys. Rev. B **28**, 4875 (1983).

²D. B. Mast, A. J. Dahm, and A. L. Fetter, Phys. Rev. Lett. **54**, 1706 (1985).

³D. C. Glatli, E. Y. Andrei, G. Deville, J. Pointreud, and F. I. B. Williams, Phys. Rev. Lett. **54**, 1710 (1985).

⁴W. Hansen, M. Horst, J. P. Kotthaus, U. Merkt, Ch. Sikorski, and K. Ploog, Phys. Rev. Lett. **58**, 2586 (1987).

⁵J. Alsmeier, E. Batke, and J. P. Kotthaus, Phys. Rev. B **40**, 12574 (1989).

⁶Ch. Sikorski and U. Merkt, Phys. Rev. Lett. **62**, 2164 (1989).

⁷A. C. Warren, D. A. Atoniadis, and H. I. Smith, Phys. Rev. Lett. **56**, 1858 (1986).

⁸M. A. Reed, J. N. Randall, R. J. Aggarwal, R. J. Matyi, T. M. Moore, and A. E. Wetsel, Phys. Rev. Lett. **60**, 535 (1988).

⁹T. P. Smith III, K. Y. Lee, C. M. Knodler, J. M. Hong, and D. P. Kern, Phys. Rev. B **38**, 2172 (1988).

¹⁰W. Hansen, T. P. Smith III, K. Y. Lee, J. A. Brum, C. M.

Knodler, J. M. Hong, and D. P. Kern, Phys. Rev. Lett. **62**, 2168 (1989).

¹¹J. Alsmeier, E. Batke, and J. P. Kotthaus, in *Proceedings of the Fourth International Conference on Modulated Semiconductor Structures*, Ann Arbor, 1989 [Surf. Sci. (to be published)].

¹²J. Alsmeier, E. Batke, and J. P. Kotthaus, in *Proceedings of the Eighth International Conference on Electronic Properties of Two-Dimensional Systems*, Grenoble, 1989 [Surf. Sci. (to be published)].

¹³W. Que and G. Kirczenow, Phys. Rev. B **38**, 3614 (1988).

¹⁴A. V. Chaplik, in *Proceedings of the Eighth International Conference on Electronic Properties of Two-Dimensional Systems*, Grenoble, 1989, Ref. 12.

¹⁵A. L. Fetter, Phys. Rev. B **32**, 7676 (1985).

¹⁶B. A. Wilson, S. J. Allen, Jr., and D. C. Tsui, Phys. Rev. B **24**, 5887 (1981).

¹⁷Ch. Sikorski, U. Merkt, and J. Alsmeier, in *Spectroscopy of Semiconductor Microstructures*, NATO Advanced Study Institutes, Series B, Vol. 206 (Plenum, New York, in press).

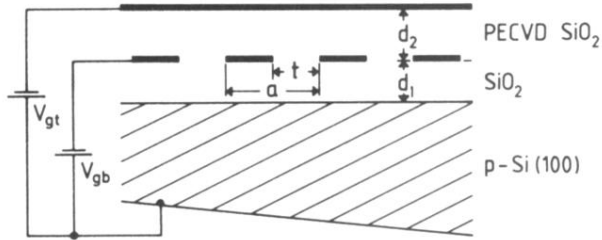
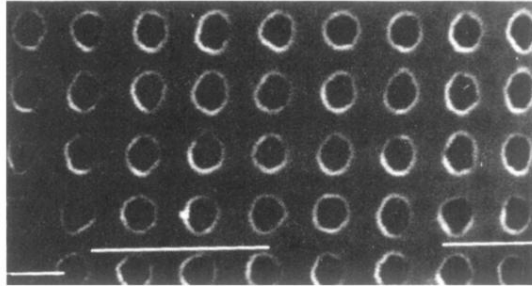


FIG. 1. Schematical cross section of a dual-gate device on Si. The top gate is a homogeneous 5-nm-thick NiCr layer, whereas the bottom gate is a NiCr mesh of periodicity $a=400$ nm embedded between a thermal ($d_1=50$ nm) and a PECVD ($d_2=150$ nm) SiO₂. The scanning electron micrograph with 1- μ m marker shows a top view of the bottom gate indicating circularly mesh opening with diameter $t \approx 150$ nm.